THERMAL AND ELECTRICAL CONDUCTIVITY MEASUREMENTS OF CDA 510 PHOSPHOR BRONZE

J. Tuttle, E. Canavan, and M. DiPirro

NASA Goddard Space Flight Center, Code 552 Greenbelt, Maryland, 20771, USA

ABSTRACT

Many cryogenic systems use electrical cables containing phosphor bronze wire. While phosphor bronze's electrical and thermal conductivity values have been published, there is significant variation among different phosphor bronze formulations. The James Webb Space Telescope (JWST) will use several phosphor bronze wire harnesses containing a specific formulation (CDA 510, annealed temper). The heat conducted into the JWST instrument stage is dominated by these harnesses, and approximately half of the harness conductance is due to the phosphor bronze wires. Since the JWST radiators are expected to just keep the instruments at their operating temperature with limited cooling margin, it is important to know the thermal conductivity of the actual alloy being used. We describe an experiment which measured the electrical and thermal conductivity of this material between 4 and 295 Kelvin.

KEYWORDS: phosphor bronze, Wiedemann-Franz, electrical resistivity, thermal conductivity.

INTRODUCTION

Electrical wiring for cryogenic systems is typically optimized to meet conflicting thermal and electrical performance requirements. Usually there is a need to limit heat conduction from a cryostat's warm shell to the cold stages, which drives the design toward small diameter and high resistance wires. Stainless steel wire is very strong and has a relatively high electrical and thermal resistivity. In many cases where currents are very low it is the ideal wire to minimize heat conduction. However, some circuits have electrical resistance limits which can result in impractically large stainless steel wire diameters. Wires that carry relatively high currents must have low electrical resistances to avoid excessive ohmic heating. Copper has some drawbacks in cryogenic systems. Its

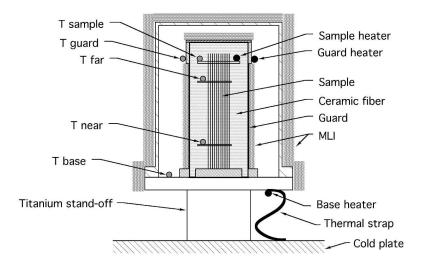


FIGURE 1. The test apparatus in which both the electrical resistivity and thermal conductivity measurements were performed.

high thermal conductivity necessitates small wire diameters, but its low strength makes small wires impractical, particularly in a space-flight application. The thermal conductivity of commonly used copper has a negative slope between about 40 Kelvin and room temperature. For a wire cooled predominantly by conduction to the ends, a negative slope means that as the wire heats, cooling of the center section becomes poorer, leading to greater temperature rise. A good alternative wire material is a relatively low resistivity alloy with a monotonically rising thermal conductivity, such as phosphor-bronze.

The James Webb Space Telescope (JWST) is a cryogenic system requiring an optimized wiring design for its instrumentation. Its wiring harnesses run over a short distance from a room-temperature electronics box to an instrument stage which is radiatively cooled to about 40 Kelvin. Due to the T^4 dependence of radiation, cooling power at this temperature is limited, and it is critical to limit the heat flow to the instruments. The heat conducted by these harnesses represents a large fraction of the total parasitic heat load into the stage. In order to meet thermal, electrical, mass, wire size and reliability requirements, most of the conductors were made of phosphor bronze. In fact, thermal conduction through phosphor bronze wires represents a large fraction of the total heat conduction. Thus, the wire sizes must be optimized based on a fairly precise knowledge of the wire's material properties.

Phosphor bronze samples vary significantly in their material constituents and thus their thermal and electrical properties. Samples tested at NASA have had a wide range of room temperature electrical resistivities. Japanese researchers have found that the electrical and thermal conductivity of phosphor bronze depend strongly on the amount of tin and phosphorous in the alloy [1]. To reduce this uncertainty vendors use a standard specification known as CDA-510 phosphor bronze, which allows 4.2 - 5.8% tin and 0.03 - 0.35% phosphorous [2]. However, the Japanese data indicate that these tin and phosphorous ranges lead to significant variations in thermal conductivity and electrical resistivity over the temperature range below 300 Kelvin. Thus, in order to evaluate the JWST wiring, we measured both the thermal conductivity and electrical resistivity of phosphor bronze wire taken from a sample of the purchased flight cabling.

EXPERIMENTAL TECHNIQUE

The apparatus used in this experiment is shown in FIGURE 1. We measured the

electrical resistance of a 848 mm long sample of 0.249 mm diameter phosphor bronze CDA 510 wire which was coiled around and taped to our thermal conductivity rig's base plate, inside a cryostat cooled by a Gifford-McMahon cryocooler. A thick copper can, bolted to the base plate's outer edge, covered the sample and protected it from radiative coupling with the rest of the cryostat. The sample's voltage and current taps were wired to a Picowatt AVS-47 resistance bridge accurate to 1 m Ω . During this part of the experiment the base plate was controlled at each of a set of temperature values between 4 and 300 Kelvin. Uncertainty in these steady resistance measurements was less than +/- 1%, and systematic error due to the sample geometry was at worst +/- 1%.

The thermal conductivity sample consisted of 10 parallel 76-mm-long phosphor bronze wires extracted from the same JWST cable as the electrical resistivity sample. Their diameters, approximately 0.25 mm, were precisely measured with a micrometer. One end of each wire was clamped to the same base plate used in the electrical resistivity measurement, and the wires stood vertically in a row. A thin strip of 0.125-mm-thick copper ran perpendicular to the wires across their tops. This strip was soldered to each wire and served as the "sample-end" heat sink. A very small heater and CernoxTM thermometer were attached to this sink with GE varnish, with their leads extending upward. Two other identical copper strip heat sinks were soldered to the wires at locations between the base plate and sample-end sink. A Cernox thermometer was varnished to each of these sinks, and the sample length between them was 51 mm.

The thermal conductivity apparatus and the measurement technique have been described in detail elsewhere [3] and will be summarized here. A 31.8 mm diameter stainless steel guard can surrounded the sample. It was bolted to the base plate and was closed out at the other end with a copper cap. During the experiment the cap temperature was independently controlled the same setpoint temperature as that of the sample-end. The guard's design was such that its temperature profile matched that of the sample. The resulting lack of any radial temperature difference between the sample and guard minimized radiative heat leaks from the sample. In addition, the volume between the sample and guard was filled with a fibrous insulation material (FiberfraxTM). The measured thermal conductivity of this material is proportional to T^3 and was much lower than phosphor bronze's thermal conductivity, even at room temperature [4].

The five temperatures were read out with Cryogenic Control Model 32B Temperature Controllers. These devices also provided three independent "P, I" control loops for the base plate, sample-end and guard-end temperatures. The current through and voltage across the sample-end thermometer were monitored with Kiethley 2000 6.5 digit multimeters.

A LabVIEWTM program controlled the experiment. It read the five thermometers (base plate, guard-end, sample-end, and two intermediate sample thermometers) and the sample heater's current and voltage 2.5 times per second. Once every five minutes it performed a linear regression on the data from each thermometer and the heater power. If the temperature and power slopes were zero to within the uncertainty of the fit and if the difference between the average temperatures and the corresponding set points were less than the standard deviation, then the system was considered to be in a steady state. If not, the program flushed its buffers and began a new five minute monitoring period. When the system was steady, the five temperatures and the sample heater power average values over the final five minute interval were recorded, along with their standard deviations. Then a new set of control temperatures was loaded for the next measurement.

For each experimental average temperature value, the power was measured at four different temperature gradients. To set up these gradients, the sample-end and guard-end temperatures were raised and the base temperature lowered by equal amounts relative to

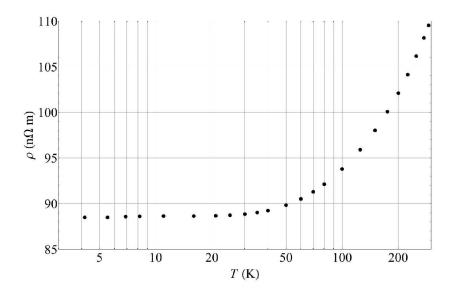


FIGURE 2. The measured electrical resistivity vs. temperature for a phosphor bronze CDA 510 wire from a sample of JWST instrument cabling.

the average temperature. A linear regression was applied to the steady-state power versus ΔT , the difference between the two intermediate sample temperatures. The slope and the sample geometry were used to compute the thermal conductivity. Using the slope from several temperature gradients eliminated systematic error due to small thermometer calibration offsets or constant heat leaks into or out of the sample. Random error in the temperature measurements was negligible, typically below 3 ppm. Random error in the power measurement was somewhat larger, but well below 1%. Maximum residuals to the linear fit were typically < 10⁻⁴ of the maximum power. Systematic uncertainty, mainly due to the sample geometry, was about +/- 1%.

Despite its very low thermal conductivity, the insulation had a relatively large cross section and conducted 13% as much heat axially as did the sample at 300 K. However, the vast majority of the insulation-conducted heat came from the guard, rather than the sample. A finite element thermal model of the experiment showed that well below one percent of the heat applied to the sample's warm end leaked into the insulation.

RESULTS AND ANALYSIS

The measured electrical resistivity ρ as a function of temperature is shown in FIGURE 2. At low temperatures it has a temperature-independent value of about 88 n Ω ·m. Above 40 Kelvin the ρ shows a near linear weak temperature dependence. The residual resistance ratio RRR = R_{300K}/R_{4.2K} is 1.24. This value is low compared to that of even the most work-hardened pure metals, but it is high compared to that of high-resistivity alloys. In comparison, Hastelloy has a low-temperature resistivity of 122 n Ω m and a RRR value of 1.03 [5]. Another alloy with a similar resistivity is aluminum 2024-T4. It has a low-temperature resistivity of about 30 n Ω m, and its RRR is about 2.0 [6].

FIGURE 3 shows the measured thermal conductivity κ as a function of temperature. Our results are shown in circles. The line through these points is a fit to the expression:

$$\ln(\kappa) = \sum_{n=0}^{\infty} A_n [\ln(T)]^n$$
(1)

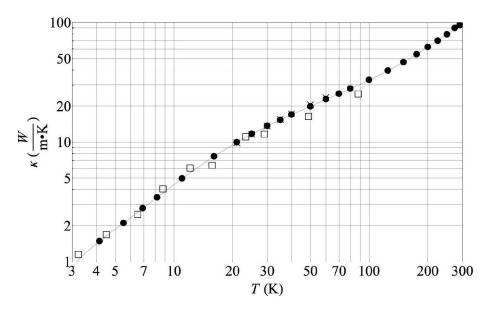


FIGURE 3. Thermal conductivity of phosphor bronze. Solid circles are from this work, using CDA 510 material taken from a JWST cable sample. ×'s are also from this work, but without using the guard can and insulation. Open squares are from Zavaritskii & Zeldovich, 1956.

The fit coefficients are given in TABLE 1. The residuals indicate no systematic deviations from the data, and the fit matches all data points to better than 0.6 percent.

Additional points, shown as \times 's, are data taken from a preliminary run with the same sample and apparatus but without installing the guard or insulation. Taken for JWST engineering purposes, these data show that guard and insulation are necessary for accurate measurements with this sample above about 40 Kelvin. The square symbols on the graph are phosphor bronze data from Zavaritskii and Zeldovich [7]. These data agree well our own below 25 Kelvin, but at higher temperatures they are systematically lower than ours.

Wiedemann-Franz Law

The total thermal conductivity of metals can be written $\kappa = \kappa_E + \kappa_G$, where κ_E is the thermal conductivity due to electron conduction and κ_G is due to phonon conduction. In pure metals $\kappa_E \gg \kappa_G$. Both at high and low temperatures they obey reasonably well the Wiedemann-Franz law, which states that $\kappa_E = L_0 T/\rho$. Here ρ is the electrical resistivity, T is the temperature, and L_0 is the Lorenz constant (approximately equal to 2.44 × 10⁻⁸ W Ω/K^2). The law breaks down at intermediate temperatures where the electron scattering is not entirely elastic, reducing the thermal conductivity to below the Wiedemann-Franz prediction for a given electrical conductivity [8,9]. The thermal conductivity of pure aluminum samples (RRR = 100) can be as low as half the predicted value at 100 Kelvin [6]. For pure copper cold-drawn to 26% of its original cross sectional area (RRR = 130), κ also dips to as low as 50% of the prediction, but at about 45 Kelvin. The κ of annealed pure copper (RRR = 1600) is as low as one third the prediction at about 25 Kelvin [10].

For alloys, where electron conduction is strongly suppressed by scattering, κ_G can be

A ₀	A ₁	A ₂	A ₃	A ₄	A ₅	A ₆	A ₇	A ₈
-10.9482	28.4752	-32.3378	20.9036	-8.05399	1.90329	-0.271774	0.0215998	-7.35095 ×10 ⁻⁴

TABLE 1. Fit coefficients for $\ln(\kappa) = A_0 + A_1 [\ln(T)] + A_2 [\ln(T)]^2 + ... + A_8 [\ln(T)]^8$.

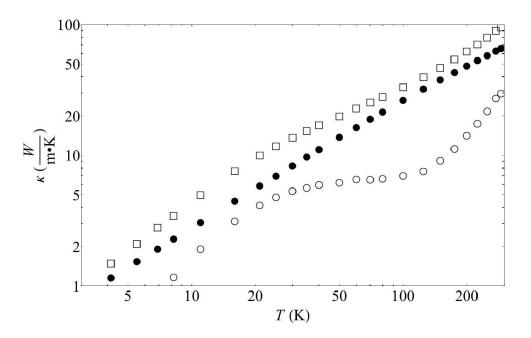


FIGURE 4. The measured total thermal conductivity, κ , of CDA 510 phosphor bronze is shown in open squares. Filled circles are the electronic contribution, κ_E , as predicted by the Wiedemann-Franz law. The open circles are the phonon contribution, calculated by subtracting κ_E from κ .

as high or higher than κ_E [11]. For high-resistivity alloys, such as Hastelloy, $\kappa_G \gg \kappa_E$ [5]. Since phosphor bronze has a much higher electrical conductivity than that of Hastelloy, it was expected that the former's κ_E , would contribute a higher percentage of the total thermal conductivity. FIGURE 4 shows the measured phosphor bronze κ , an estimate of κ_E assuming the Wiedemann-Franz law applies over the temperature range, and, $\kappa_G = \kappa - \kappa_E$. This estimate neglects the suppression of κ_E from inelastic electron scattering. Not surprisingly, the estimated κ_E is larger than κ_G over the entire temperature range studied. At temperatures above about 100 K, κ_E dominates the thermal conductivity.

FIGURE 5 shows the Lorenz ratio L/L_0 for our phosphor bronze samples. Here L is an effective Lorenz number computed by inserting κ in place of κ_E in the Wiedemann-Franz law, and L_0 is the Lorenz constant. Over the studied temperature range L/L_0 is always greater than 1 due to the significant contribution of κ_G . The shape of this curve probably results from non-Wiedemann-Franz behavior of κ_E and the unknown temperature dependence of the actual κ_G .

It is interesting to compare this L/L_0 with that computed for other alloys. The L/L_0 curve for aluminum 2024-T4, with a low temperature ρ only about one third that of our phosphor bronze sample, has a low temperature value less than 1.1 and a minimum below 1.0 near 100 Kelvin [6]. Hastelloy, which is 40% more resistive at low temperatures than our sample, has a 5 Kelvin Lorenz ratio of about 12, which monotonically decreases to about 2.6 at room temperature [5].

Implications for Cryogenic Wiring

In designing and evaluating cryogenic wiring systems, it is rare that one finds thermal data for precisely the available wire material. An alloy's chemical makeup or a pure metal's RRR value usually differ from exactly what is in the literature. Even less commonly found are thermal conductivity and electrical resistivity data for exactly the same material. When finding only one of these parameters for a given metal, it is tempting

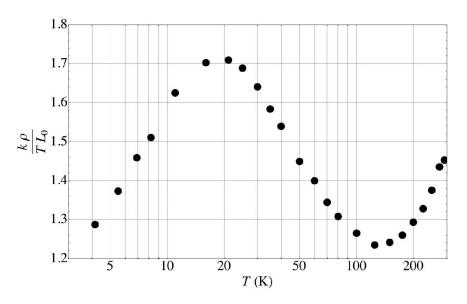


FIGURE 5. The Lorenz ratio L/L_0 , for phosphor bronze CDA 510, Here L is a Lorenz number calculated with the Wiedemann-Franz law using the total thermal conductivity, and L_0 is the fundamental Lorenz constant computed from the elastic-scattering-only electronic thermal conductivity.

to estimate the other by assuming that $\kappa = \kappa_E$ using the Wiedemann-Franz law to relate κ_E and ρ . This is a risky approach, however, as it over-predicts κ over a wide temperature range for pure metals and generally under-predicts κ everywhere for alloys. If it were valid for all pure metals and alloys, in terms of thermal performance alone they would all be equally suitable for use in wires carrying significant current (ignoring thermal radiation). Given the current carried by a wire and its end point temperatures, there would be a single minimum achievable heat flow out the cold end. For each metal or alloy, one optimum area/length ratio would produce this same minimum value. For wires spanning a large temperature range, it might be necessary to vary the diameter along the length in order to achieve this optimization.

We used a simple iterative thermal model to explore the optimization of 50 cm long wires carrying a steady one amp current. The model had only ten nodes, ignored radiation, and used curve fits of the thermal conductivity and electrical resistivity data for Hastelloy [5], phosphor bronze (this work), and 26% drawn copper [10]. For each material we calculated the heat at the cold end, held at 4 Kelvin, for a series of different warm end temperatures. At each warm end temperature the wire diameter was varied until the minimum heat value was found.

FIGURE 6 shows the results of these calculations. For a current lead running from 20 to 4 Kelvin, an optimized Hastelloy wire delivers almost four times more heat than an ideal copper wire. Phosphor bronze fares better than Hastelloy but is still about 50% worse than copper. If the wire runs from 300 to 4 Kelvin, the Hastelloy and phosphor bronze deliver about two times and 20% more heat than copper, respectively. Considering the need to over-design copper wires to avoid the potential for thermal run-away, phosphor bronze might actually be a better choice in the latter case. However, heavily-alloyed metals such as Hastelloy, and most likely stainless steel, would be poor choices.

CONCLUSION

The measured electrical resistivity and thermal conductivity of phosphor bronze CDA 510 will be useful in evaluating the space-flight wiring of JWST. The relationship between

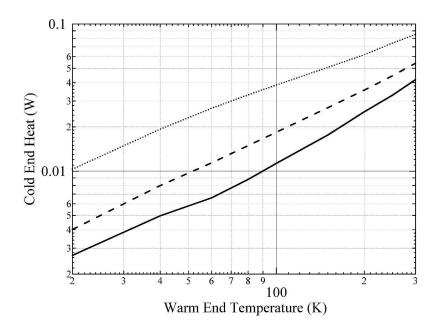


FIGURE 6. The minimum possible heat load at the cold end of an 50 cm long wire conducting 1 amp of current with cold end held at 4 Kelvin. The wire diameter has been optimized at each warm end temperature to minimize the cold end load. Radiation is ignored. The solid line is for 26% drawn copper[10], the large-dash line is for phosphor bronze CDA-510 (this work), and the dotted line is for Hastelloy C-276TM[5].

these parameters is not very well described by the Wiedemann-Franz law, since κ includes a significant contribution from phonons. The results of this work and of other work cited here indicate that this law should be used very cautiously in estimating κ or ρ for either pure metals or alloys. In wires where Joule heating is important, phosphor bronze is a good choice, while heavily-alloyed metals should be avoided. A low-RRR formulation of pure copper might be even better than phosphor bronze in certain applications.

ACKNOWLEDGEMENTS

This work was supported by NASA's James Webb Space Telescope program. We thank Tom Hait for his help in setting up the test apparatus, and John Francis for his finite-element thermal modeling.

REFERENCES

- 1. Kosaka, K., Yamanaka, N., Matsukawa, M., and Yoshizawa, M., J. of JCBRA, 39, pp. 197-201 (2006).
- 2. ASTM Standard B 159/B 159M, "Standard Specification for Phosphor Bronze Wire."
- Canavan, E. R. and Tuttle, J. G., "Thermal Conductivity and Specific Heat Measurements of Candidate Structural Materials for the JWST Optical Bench," in Advances in Cryogenic Engineering 52A, edited by U. B. Balachandran et al., AIP, New York, 2006, pp. 233-240.
- 4. Moore, J. P., Williams, R. K., and Graves, R. S., Rev. of Sci. Instr., 45(1), pp. 87-95 (1973).
- 5. Lu, J., Choi, E. S., and Zhou, H. D., J. Appl. Phys., 103 pp. 064908-1-6 (2008).
- 6. Powell, R. L., Hall, W. J., and Roder, H. M., J. Appl. Phys., 31 pp. 496 -503 (1960).
- 7. Zavaritskii, N.V. and Zeldovich, A.G., Sov. Phys. Tech. Phys. 1 pp. 1970-1974 (1956).
- 8. Ashcroft, N. and Merman, N. D., Solid State Physics, Saunders, Philadelphia, 1976.
- 9. Ziman, J. M, Principles of the Theory of Solids, Cambridge, 1972, pp. 231-235.
- 10. Powell, R. L., Roder, H. M., and Hall, W. J., Phys. Rev., 115 pp. 314-323, (1959).
- 11. Kittel, C., Introduction to Solid State Physics, Fifth Edition, Wiley, New York, 1976.